JOURNAL OF PHYSICAL ORGANIC CHEMISTRY
J. Phys. Org. Chem. 2007; **20:** 167–179
Published online in Wiley InterScience
(www.interscience.wiley.com) DOI: 10.1002/poc.1142

Nucleophilic reactivity of aniline derivatives towards the nitroso group†

Gabriel da Silva, Eric M. Kennedy* and Bogdan Z. Dlugogorski

Process Safety and Environment Protection Research Group, School of Engineering, The University of Newcastle, Callaghan, NSW 2308, Australia

Received 31 July 2005; revised 2 March 2006; accepted 20 March 2006

ABSTRACT: This study investigates the reactivity of the electrophilic nitroso group towards nucleophilic aniline derivatives from various nitrosating agents. A relationship between the rate of nitrosation and Edwards' nucleophilic parameter (E_n) is disclosed, indicative of a transition state that is mostly product-like in nature with respect to cleavage of the nitroso bond in the nitrosating agent. A similar relationship based on the work of Marcus provides a considerably better explanation of the data. Through application of the Marcus equation, the free energy change of reaction is calculated for the nitrosation reactions studied, which in turn is applied to develop an equation linking the free energy of formation of a nitrosamine and its corresponding protonated amine. This equation accounts for the often-observed Brønsted relationships in nitrosation reactions. The intrinsic barrier to reaction is estimated to be 10 kJ mol^{-1}, indicating that the main impedance to nitrosation arises from the unfavourable reaction thermodynamics. However, for the nitrosation of aniline derivatives substituted with π-electron withdrawing groups, an unbalancing of the transition state results in an increased intrinsic barrier, of the order of 19 kJ mol^{-1}. For electronic-effect aniline derivatives, a More O'Ferrall–Jencks diagram shows the nitrosation transition state to be synchronously well balanced between reactants and products. This diagram also confirms that the reaction follows a concerted mechanism. The nitrosation of resonance-stabilised aniline derivatives is somewhat less synchronous, however, due to delocalisation of the lone electron pair on the amino group, induced by π electron withdrawing substituents. Transition states were located according to the theory of harmonic parabolic wells. The results of these calculations agreed with transition state locations predicted using linear free energy relationship techniques. A method is developed which approximates free energy profiles by treating the product and reactant free energy wells as harmonic parabola, while the free energy profile around the transition state is taken as the parabolic barrier to the product and reactant energy wells. Applying this technique, free energy profiles for electronic-effect and resonance-stabilised aniline nitrosation are predicted, utilising measured kinetic values and predicted thermodynamic properties. We couple the simulated free energy profiles with their corresponding More O'Ferrall–Jencks diagrams in order to elucidate the three-dimensional reaction path traversed between reactants and products, in terms of both structure and energy. We also demonstrate that the nitrosonium ion behaves as a soft acid, and should therefore undergo covalent frontier-orbital controlled bonding.

Supplementary electronic material for this paper is available in Wiley Interscience at http://www.interscience.wiley.com/suppmat/0894-3230/suppmat/

KEYWORDS: LFER; Marcus equation; S_N2 mechanism; nitrosation; free energy profile; principle of non-perfect synchronisation; harmonic parabolic wells

INTRODUCTION

In recent times, reactions involving nitroso group transfer have generated a great deal of interest. This interest has largely risen out of the discovery of the vital role that nitric oxide plays in the regulation of numerous physiological functions.[1] In addition, nitrosation reactions are of pertinence due to the highly toxic and carcinogenic properties of many *N*-nitrosamines,[2] while they are also important in several industrial processes.[3] Much effort has been directed at determining factors which affect the rate of nitroso group transfer, consistent with the significance of nitrosation reactions. Many of these studies have made use of *ab initio* techniques and thermodynamic cycles to estimate bond dissociation energies (BDEs),[4] or to study the nature of nitrosation transition states and the intrinsic barrier to reaction.[5] Another common approach to analysing nitroso reactivity has been to use linear free energy relationships (LFER).

**Correspondence to:* E. M. Kennedy, School of Engineering, The University of Newcastle, Callaghan, NSW 2308, Australia.
E-mail: Eric.Kennedy@newcastle.edu.au
†Presented in part at the 19th Royal Australian Chemical Institute Organic Conference, Lorne, Australia, 2003.

The use of LFER has centred chiefly around the construction of Brønsted-style plots, in which ln$k$ is plotted against pK_a, to assess the relative importance of substrate basicity on the rate of reaction. However, the results of these studies are often contradictory, in that the existence of good Brønsted correlations have[6] and have not been reported,[7,8] for various systems. Additionally, reactivity has been correlated with other nucleophilic parameters such as Ritchie's N_+ parameter,[8,9] vertical ionisation potential,[7] and the Hammett[6e,10] and Pearson[11] parameters.

With respect to nitrosation reactions, a great deal of kinetic measurements exist for the reaction of aniline and its derivatives, but relatively little is known about factors affecting the reactivity of these systems. This is in spite of the fact that aromatic nitrosamines tend to be highly carcinogenic, and are relatively stable in solution (as opposed to most primary aliphatic nitrosamines). Aromatic nitrosamines have also been shown to affect transnitrosation to other substrates,[12] opening further pathways for the formation of a wide range of toxic compounds. The two factors of basicity and nucleophilicity are known to affect the reactivity of aniline and its derivatives towards nitroso-bearing species. Stedman and Whincup[6f] have observed linear relationships between the rate of aniline nitrosation and pK_a, demonstrating that reactivity increases with increasing basicity of the amine. In addition, Williams[13] observed that the reactivity of aniline (among other substrates) increases as the equilibrium constant of the corresponding nitrosating agent decreases. Recently, da Silva *et al.*[14] showed that these equilibrium constants are related to the nucleophilic strength of the nitrosating agent through Edwards' nucleophilic parameter, E_n. Thus, we see that nitroso group reactivity towards aniline-type compounds increases with increasing amine basicity and with increasing nitrosating agent electrophilicity (i.e. decreasing nucleophilicity).

The factors affecting nitroso reactivity towards aniline and its derivatives remain relatively poorly understood, despite the considerable importance of this class of reactions. Previous researchers have identified the effects of basicity and nucleophilicity as being important, though they have not quantified or mechanistically described either effect. As such, this study attempts to quantify the factors affecting the reactivity of the nitroso group towards aniline and its derivatives, using LFER. We then extend the conclusions drawn from this system to incorporate nitrosation reactions in general.

EXPERIMENTAL DATA

The present study is concerned with reactions carried out under mildly acidic conditions, where nitrosation proceeds through the initial formation of an electrophilic nitrosating agent, ONX (Eqn 1), and subsequent reaction of this nitrosating agent with a nucleophilic substrate (S), according to Eqn (2).[15] Under such conditions, nitrosation by the species ON^+ (H_2ONO^+) is considered negligible. Nitrosating agents are formed from the equilibrium reaction of nitrous acid with certain nucleophilic catalysts, including chloride,[16] bromide,[17] thiocyanate,[6f] iodide,[18] thiourea[19] and thiosulphate,[20] according to Eqn (1). In solutions of nitrous acid, the nitrosating agent dinitrogen trioxide is also formed,[21] where dissociated nitrite ions act as the nucleophilic species. Common substrates that undergo nitrosation include amines, thiols and hydrocarbons, among others.

$$HNO_2 + X^- + H^+ \overset{K_{ONX}}{\rightleftharpoons} ONX + H_2O \qquad (1)$$

$$ONX + S \overset{k_N}{\rightarrow} ONS^+ + X^- \qquad (2)$$

Rate constants for the nitrosation of aniline derivatives by a range of nitrosating agents, according to the above mechanism, have been compiled from numerous sources,[10e,14,16,17,22] and are reproduced in Table 1. In some instances, the quoted rate constants correspond to averages of values from several literature sources. In our study, we plan to use these experimental values to examine the reactivity of the nitroso group towards aniline-type compounds. The experimental data cover a range of primary aromatic amines substituted in the *ortho*, *meta* and *para* positions, as well as one secondary amine. Also included in the table are experimental measurements for the nitrosation of 1-naphthylamine compounds, which contain two aromatic rings. All rate constants quoted in this study are at 25°C.

Table 1 shows that k_N values for nitrosation via the reactive nitrosating agents ONCl and ONBr appear to approach a maximum value of around $5 \times 10^9\,M^{-1}\,s^{-1}$. This value represents the encounter controlled limit,[22i,j] at which chemical reactivity ceases to control, and molecular diffusion dominates, and as such we have removed these measurements. It was shown by da Silva *et al.*[23] that there is only a limited transition regime between diffusion and reaction control, indicating that, in general, measured rate constants lie completely within one regime. As such, we have assumed that any rate constant below $9 \times 10^8\,M^{-1}\,s^{-1}$ is completely unaffected by encounter control.

DISCUSSION

We begin our analysis of nitroso reactivity with an exploration of the thermodynamics of nitrosation, as we attempt to describe the free energy change of nitrosation based upon known kinetic information. Subsequently, we perform an analysis of Brønsted-style relationships in the nitrosation of aniline derivatives. The developed thermodynamic models will be used to clarify the nature of such relationships, alternative relationships will be

DOI: 10.1002/poc

Table 1. Rate constants (k_N, $M^{-1}s^{-1}$) for the nitrosation of aniline derivatives by various nitrosating agents at 25°C

	ONCl	ONBr	N_2O_3	ONSCN	ONI	$ON^+SC(NH_2)_2$	$ONS_2O_3^-$
1-naphthylamine	2.22×10^9	3.70×10^9	–	3.82×10^8	–	2.45×10^6	–
4-bromo-1-naphthylamine	1.38×10^9	1.72×10^9	–	3.35×10^7	–	2.78×10^5	–
4-chloro-1-naphthylamine	2.08×10^9	2.60×10^9	–	8.26×10^7	–	4.45×10^5	–
4-cyano-1-naphthylamine	–	6.21×10^7	–	–	–	–	–
4-nitro-1-naphthylamine	3.69×10^8	2.16×10^7	–	2.29×10^5	–	1.89×10^3	–
7-hydroxy-1-naphthylamine	1.24×10^{10}	4.48×10^9	–	4.73×10^8	–	4.26×10^6	–
Aniline	2.8×10^9	2.2×10^9	7.5×10^8	1.87×10^8	2.6×10^6	1.3×10^6	2.2×10^2
m-Chloroaniline	1.6×10^9	–	9.6×10^7	–	–	–	–
m-Methoxyaniline	3.2×10^9	2.2×10^9	–	2.0×10^7	1.9×10^6	6.3×10^5	–
m-Methylaniline	2.7×10^9	5.27×10^9	8.2×10^8	–	–	–	–
m-Nitroaniline	1.2×10^9	1.1×10^8	–	–	–	–	–
N-Methylaniline	3.0×10^9	4.1×10^9	4.0×10^8	2.8×10^8	–	–	1.2×10^4
o-Chloroaniline	1.2×10^9	–	1.4×10^7	–	–	–	1.6×10^0
o-Methylaniline	2.4×10^9	3.75×10^9	4.2×10^8	–	–	–	–
p-Carboxyaniline	1.1×10^9	4.3×10^8	–	1.4×10^6	8.8×10^4	1.8×10^4	–
p-Chloroaniline	2.0×10^9	2.5×10^9	2.8×10^8	8.2×10^7	2.9×10^6	4.0×10^5	2.0×10^1
p-Methoxyaniline	5.5×10^9	3.0×10^9	–	7.46×10^8	2.6×10^7	1.6×10^7	–
p-Methylaniline	3.5×10^9	2.7×10^9	1.9×10^9	4.08×10^8	–	5.0×10^6	–
p-Nitroaniline	2.4×10^8	4.3×10^7	–	–	–	–	–
p-Sulphamidoaniline	1.8×10^8	4.4×10^7	–	7.3×10^4	–	2.0×10^2	–
p-Sulphoaniline	1.4×10^9	9.9×10^8	–	2.0×10^6	–	5.9×10^3	–

explored, and the results analysed mechanistically. Finally, the known kinetic data and the predicted thermodynamic properties will be used, in conjunction with the mechanistic insight provided by the analysis of Brønsted and other free energy relationships, to study the transition states that occur during aniline nitrosation.

Nitrosation thermodynamics

It is well known that the kinetics of bimolecular nucleophilic substitution (S_N2) reactions, including nitrosation reactions of the form of Eqn (2), are affected by both polarisability and basicity.[24] Currently accepted theory interprets the action of polarisability as indicative of a frontier-orbital controlled reaction, forming covalent bonds, while basicity is indicative of a charge-transfer controlled reaction, forming ionic bonds.[25]

Edwards[24] utilised LFER techniques in describing the kinetic effect of polarisability and basicity with the parameters E_n and pK_a, respectively. Later, the hard and soft acids and bases (HSAB) principle qualitatively identified that the same two properties were responsible for determining the thermodynamics, as well as kinetics, of S_N2 class reactions.[26] According to the HSAB principle, acids (electrophiles) which bonded favourably with bases (nucleophiles) according to polarisability were qualitatively labelled as soft, while those that bonded favourably according to basicity were qualitatively labelled as hard. Later, Yingst and McDaniel[27] showed that a quantitative link existed between the parameters of Edwards and the HSAB principle, in that the reactions of soft bases were described largely according to E_n, and those of hard bases were described largely according to pK_a. Consequently, they interpreted the softness of a base as the ratio of the contributions of E_n and pK_a.

It has been demonstrated that equilibrium reactions involving nitroso group transfer are well described by an LFER between $\ln K_{ONX}$ and E_n.[6f] In Fig. 1, a similar relationship between $\ln K_{ONX}$ and pK_a is plotted. Evidently, no discernible relationship exists, and as such we may label the nitroso species a soft acid, according to Yingst and McDaniel's[27] interpretation of the HSAB principle. Furthermore, by observing the intimate link

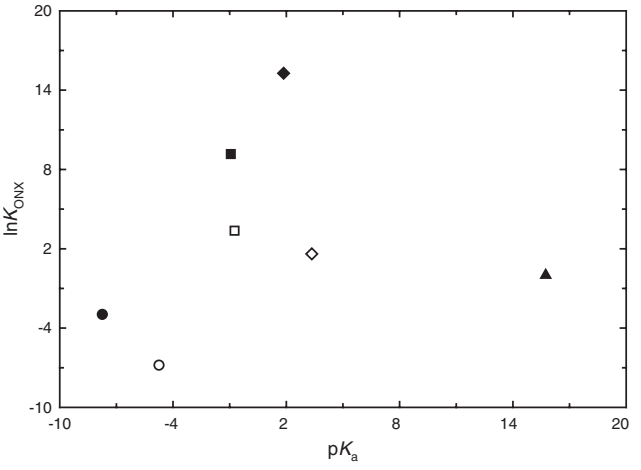

Figure 1. pK_a *versus* $\ln K_{ONX}$ for the species ONBr (●), ONCl (○), $ON^+SC(NH_2)_2$ (■), ONSCN (□), $ONS_2O_3^-$ (◆), N_2O_3 (◇) and HNO_2 (▲)

DOI: 10.1002/poc

between thermodynamic and kinetic properties,[28] we propose that the reactivity of nitroso group transfer would be dictated by polarisability, not basicity. This conclusion suggests that the reactions of the nitroso species would be frontier-controlled, with the resultant bonds being mostly covalent in nature. This agrees with the results of a recent *ab initio* study of nitroso bonding in the common nitrosating agents ONCl, ONBr, N_2O_3 and ONSCN.[4d]

According to the relationship of da Silva *et al.*,[14] Eqn (3) may be derived, which relates the free energies of formation of a nitrosating agent and its constituent nucleophile to the E_n parameter. Here, the Gibbs free energies have units of $J\,mol^{-1}$.

$$\Delta G^{o}_{f,ONX} - \Delta G^{o}_{f,X^-} = 254\,000 - 44\,400E_n \quad (3)$$

Equation (4) gives the free energy change for a typical nitrosation reaction (i.e. Eqn 2). Upon substitution of Eqn (3) into this relationship, we obtain Eqn (5), which describes the free energy change for nitrosation.

$$\Delta G^{o}_{N} = \Delta G^{o}_{f,ONS^+} + \Delta G^{o}_{f,X^-} - \Delta G^{o}_{f,ONX} - \Delta G^{o}_{f,S} \quad (4)$$

$$\Delta G^{o}_{N} = \Delta G^{o}_{f,ONS^+} - \Delta G^{o}_{f,S} + 44\,400E_n - 254\,000 \quad (5)$$

Leffler[28a] showed that the thermodynamics and kinetics for a reaction series are often related by LFER of the form of Eqn (6), where the parameter α describes the resemblance of the transition state to the reaction products, and C_1 is some constant. The application of this theory assumes that the processes involved in transition state formation develop synchronously, resulting in a balanced transition state.[29] It has previously been demonstrated that this is the case during nitroso transfer,[6b] allowing us to apply this theory.

$$\Delta G^{\ddagger} = \alpha \Delta G^{o} + C_1 \quad (6)$$

Introducing Eqn (5) into Eqn (6), the following expression is obtained.

$$\Delta G^{\ddagger}_{N} = \alpha(\Delta G^{o}_{f,ONS^+} - \Delta G^{o}_{f,S} + 44\,400E_n - 254\,000) + C_1 \quad (7)$$

For the reaction of various nitrosating agents with a single substrate the free energies of formation in Eqn (7) remain constant, thus allowing us to group together these constant terms to yield Eqn (8). This equation is similar in form to the kinetic model presented by da Silva *et al.*,[23] in that the free energy of activation is linearly proportional to E_n, and that the equation is only valid for the nitrosation of a single substrate.

$$\Delta G^{\ddagger}_{N} = 44\,400\alpha E_n + C_2 \quad (8)$$

According to the above relationship, the slope of a plot of $-\ln k_N$ against E_n (for one particular substrate) should reveal the value of α, and thus provide information as to the nature of the transition state. This plot is made in Fig. 2 for the nitrosation of aniline by a range of nitrosating agents. Excluding the encounter-controlled measurements obtained with ONBr and ONCl, a good linear relationship is observed, spanning over six units on the natural logarithmic scale, with a slope of −14.9; similar slopes have also been observed for the nitrosation of other substrates.[23,30] According to Eqn (8) the observed slope yields an α value of 0.83, indicating that the nitrosation transition state greatly resembles the reaction products. The parameter α is often taken to denote the bond order of the transition state, n_T. The bond order, n, signifies the covalent σ bond being formed between the nitroso group and the substrate, and accepts a value of unity for the fully formed bond and zero for the initial reactant state of nitrosating agent and substrate. We may only apply this description if the formation of the bond between the nitroso group and the substrate is synchronous with the destruction of the bond between the nitroso group and the nucleophile.[6b] In the case of a non-synchronous transition state, the α parameter would represent the order of the ON—X bond in the transition state, which would vary independently of the ON—S bond. In this case, we would obtain two α values, one designated $\alpha_{ON—X}$ and one $\alpha_{ON—S}$.

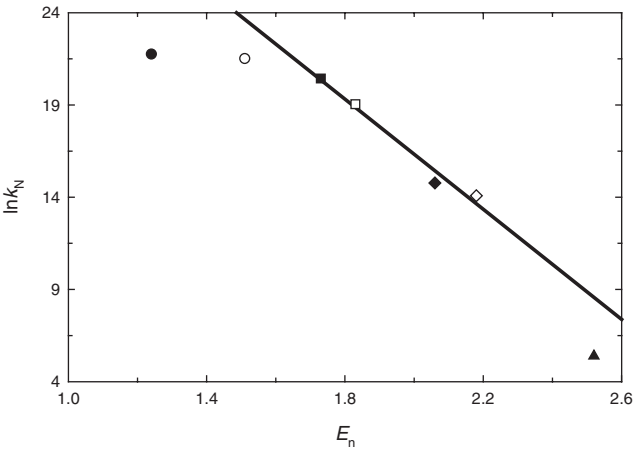

Figure 2. Relationship between E_n and $\ln k_N$ for the nitrosation of aniline via ONCl (●), ONBr (○), N_2O_3 (■), ONSCN (□), ONI (◆), $ON^+SC(NH_2)_2$ (◇) and $ONS_2O_3^-$ (▲). Linear relationship represents the Leffler equation, featuring an α value of 0.83. Experimental results for ONCl and ONBr are under encounter control, and are therefore excluded from the relationship. The experimental result for $ONS_2O_3^-$ did not conform to the Leffler equation within the tested range of reactivity

Across a wide range of values, it is known that the relationship between free energy change and the free energy of activation begins to depart from linearity. We witness this in Fig. 2, where the experimental value for nitrosation via $ONS_2O_3^-$ deviates significantly from the linear relationship (about 3 units on the logarithmic scale below the predicted value). Here, a more accurate

DOI: 10.1002/poc

description of the experimental results is provided by the electron transfer theory of Marcus,[28b,c] where the free energy relationship adopts a quadratic form. The Marcus equation is given in Eqn (9), where $\Delta G_o^{\ddagger}$ is the intrinsic barrier to reaction, and can be considered constant within a reaction series. The intrinsic barrier to reaction is analogous to the constant term in Eqn (6).

$$\Delta G^{\ddagger} = \Delta G_o^{\ddagger}\left(1 + \frac{\Delta G^o}{4\Delta G_o^{\ddagger}}\right)^2 \tag{9}$$

Substituting Eqn (5) into Eqn (9) yields Eqn (10). By fitting the global curvature of Eqn (10) to experimental measurements of $\Delta G^{\ddagger}$, the intrinsic barrier to reaction ($\Delta G_o^{\ddagger}$) can be determined, along with values for ($\Delta G^o_{f,ONS^+} - \Delta G^o_{f,S}$). In addition, the ($\Delta G^o_{f,ONS^+} - \Delta G^o_{f,S}$) values can be used with the respective E_n values to estimate the free energy change of nitrosation (ΔG_N^o) for a particular combination of nitrosating agent and substrate. In fitting the Marcus equation to the experimental data, a plot of ΔG_N^o *versus* $\Delta G_N^{\ddagger}$ was produced, and values of ($\Delta G^o_{f,ONS^+} - \Delta G^o_{f,S}$) for each substrate were varied, while simultaneously adjusting $\Delta G_o^{\ddagger}$. Within a reaction series, we assumed the intrinsic barrier to be the same for each substrate, and therefore all of the experimental results within a reaction series had to be solved simultaneously, by using an iterative technique. In each case, we fitted the quadratic equations in the least-squares sense.

$$\Delta G^{\ddagger} = \Delta G_o^{\ddagger}\left(1 + \frac{\Delta G^o_{f,ONS^+} - \Delta G^o_{f,S} + 44\,400E_n - 254\,000}{4\Delta G_o^{\ddagger}}\right)^2 \tag{10}$$

The experimental measurements of Table 1 have been divided into two separate reaction series, based upon the nature of the substrate. The first series included only those substrates whose substituents operate through electronic (inductive) effects; this series includes the bulk of the amines. The second series only contains those compounds whose substituents are considerably π electron withdrawing, in addition to being σ withdrawing. This second series contains the substrates 4-cyano-1-naphthylamine, 4-nitro-1-naphthylamine, *p*-nitroaniline, *p*-sulphamidoaniline and *p*-sulphoaniline. Note that *m*-nitroaniline was considered as an electronic effect substrate, due to the nitro group being positioned in the deactivating meta position. The above division was made because π electron withdrawing substituents are capable of inducing mechanistic change on the current reaction series, through resonance interaction with the π donating amino group. Such mechanistic change is often witnessed as LFER deviations.[31] By dividing all of the tested substrates into two reaction series, we are able to examine whether or not there is, in fact, any significant mechanistic change between the two series of reactants.

The intrinsic barrier to reaction has been determined for both reaction series, by performing the analysis of the experimental results according to the solution technique described above. For the electronic effect aniline derivatives, the intrinsic barrier was determined as $10 \pm 1.5\,kJ\,mol^{-1}$. The quoted error was calculated as the average difference between the experimental and the predicted $\Delta G^{\ddagger}$ values. The determined intrinsic barrier represents a relatively small contribution to the overall barrier to reaction, indicating that the main impedance to the rate of nitrosation is thermodynamic, and does not significantly depend upon the intrinsic reactivity of the system. According to the theory of non-perfect synchronisation, the magnitude of the intrinsic barrier suggests that the reaction follows a concerted pathway, with a transition state that is synchronously balanced between reactants and products.[31a,32] Intrinsic barriers were determined individually for each of the resonance-stabilised substrates, and it was found that the intrinsic barriers for nitrosation of *p*-sulphamidoaniline and *p*-sulphoaniline were lower than those for 4-nitro-1-naphthylamine and *p*-nitroaniline, yet still higher than that of the electronic effect substrates. When the data for *p*-sulphamidoaniline and *p*-sulphoaniline were solved simultaneously, an intrinsic barrier of $13 \pm 0.9\,kJ\,mol^{-1}$ was obtained, while for the other resonance-stabilised aniline derivates a barrier of $19 \pm 1.0\,kJ\,mol^{-1}$ was found. We believe that this result indicates incomplete resonance development for *p*-sulphamidoaniline and *p*-sulphoaniline, due to their mildly π electron withdrawing substituents. Subsequently, we will consider these two substrates individually in further analysis. The intrinsic barrier for the resonance-stabilised aniline derivatives of $19\,kJ\,mol^{-1}$ is considerably larger than that determined for the electronic-effect anilines. According to the theory of non-perfect synchronisation, a less concerted pathway is expected for the resonance-stabilised aniline derivatives than with the electronic effect derivatives. However, one should remember that $19\,kJ\,mol^{-1}$ is still not a large intrinsic barrier when compared with many other organic reaction mechanisms. A sample plot of the Marcus equation for the nitrosation of aniline, using the intrinsic barrier determined above, is shown in Fig. 3. This figure demonstrates that we have largely accounted for the departure from linearity encountered with the Leffler equation. The free energy changes computed for each of the reactions using the three intrinsic barriers are provided in Table 2.

Interestingly, the Marcus equation suggests that the free energy change for most of the nitrosation reactions analysed is small and positive, indicating that equilibrium would lie, in general, slightly in favour of the reactants. This is in spite of the fact that *N*-nitrosation reactions of the type studied here are known to be thermodynamically

DOI: 10.1002/poc

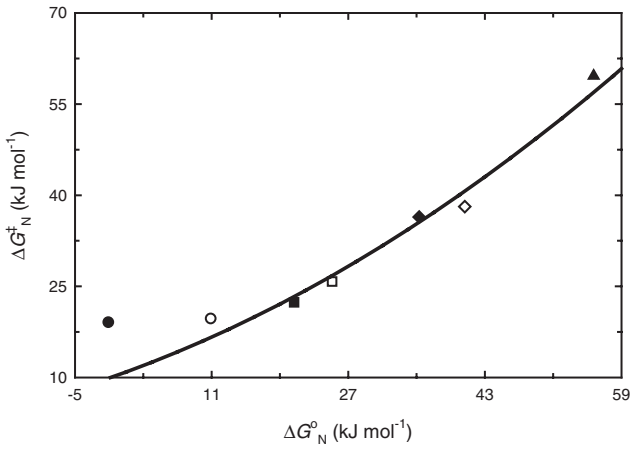

Figure 3. Relationship between ΔG^{o}_{N} and $\Delta G^{\ddagger}_{N}$ for the nitrosation of aniline via ONCl (●), ONBr (○), N_2O_3 (■), ONSCN (□), ONI (◆), $ON^{+}SC(NH_2)_2$ (◇) and $ONS_2O_3^{-}$ (▲). Solid line represents a plot of the Marcus equation, featuring an intrinsic barrier to reaction of 10 kJ mol^{-1}. The encounter controlled experimental results of ONCl and ONBr are excluded from the Marcus equation

favoured, with the equilibrium position lying well to the right. However, this thermodynamic driving force does not arise from the nitrosation step itself, but from the subsequent rapid deprotonation of the *N*-nitrosamine, which effectively drives the reaction towards product formation. This interpretation of the reaction mechanism supports the previous conclusion that the main barrier to reaction arises from the unfavourable thermodynamics of the system, and not the intrinsic barrier to reaction.

The magnitude of the intrinsic barriers determined according to curvature measurements are known to vary substantially, depending upon the method by which they are calculated. While global curvature methods, such as that employed here, are more accurate than local curvature methods, small errors in the experimental data may still introduce significant discrepancies into the final result.[33] For example, some of the results obtained in the literature show that intrinsic barriers determined via curvature measurements may be significantly smaller than the actual value of the barrier.[34] The intrinsic barrier determined here agrees reasonably well with a previous estimate (15 kJ mol^{-1}),[23] obtained by ignoring the curvature described by the Marcus equation; this agreement helps validates our analytical methodology. With respect to the intrinsic barriers determined for the resonance-stabilised substrates, it is not uncommon for substituent variations to result in changes in the intrinsic barrier.[35] However, we do recognise that the estimate for the resonance-stabilised barriers is less accurate than the electronic effect barrier, as these barriers were determined for fewer substrates.

The thermodynamic evidence presented above (Table 2) suggests that the nitroso product with which we are concerned is actually an unstable reaction intermediate, similar to the Wheland adducts observed by Hubig and Kochi.[36] The similarity in energy levels between the transition state and the reaction intermediate indicates that, according to the Hammond postulate, they

Table 2. Free energy change (ΔG^{o}_{N}, kJ mol^{-1}) for the nitrosation of aniline derivatives by various nitrosating agents, calculated using the Marcus equation with an intrinsic barrier of 10 kJ mol^{-1}

	ONCl	ONBr	N_2O_3	ONSCN	ONI	$ON^{+}SC(NH_2)_2$	$ONS_2O_3^{-}$
1-naphthylamine	–	–	–	21.2	–	36.7	–
4-bromo-1-naphthylamine	–	–	–	27.5	–	43.0	–
4-chloro-1-naphthylamine	–	–	–	22.9	–	38.4	–
4-cyano-1-naphthylamine	–	17.9	–	–	–	–	–
4-nitro-1-naphthylamine	11.0	23.0	–	37.2	–	52.7	–
7-hydroxy-1-naphthylamine	–	–	–	20.0	–	35.5	–
Aniline	–	–	20.7	25.1	35.3	40.6	55.7
m-Chloroaniline	–	–	26.0	–	–	–	–
m-Methoxyaniline	–	–	–	26.9	37.1	42.4	–
m-Methylaniline	–	–	19.1	–	–	–	–
m-Nitroaniline	–	15.6	–	–	–	–	–
N-Methylaniline	–	–	16.8	21.3	–	–	51.9
o-Chloroaniline	–	–	32.4	–	–	–	67.4
o-Methylaniline	–	–	21.3	–	–	–	–
p-Carboxyaniline	–	20.7	–	34.9	45.1	50.5	–
p-Chloroaniline	–	–	23.6	28.0	38.2	43.5	58.6
p-Methoxyaniline	–	–	–	18.0	28.3	33.6	–
p-Methylaniline	–	–	–	19.9	–	35.5	–
p-Nitroaniline	9.56	21.6	–	–	–	–	–
p-Sulphamidoaniline	17.8	29.8	–	44.0	–	59.6	–
p-Sulphoaniline	–	21.6	–	35.8	–	51.3	–

An intrinsic barrier of 19 kJ mol^{-1} was used for the resonance-stabilised aniline derivatives and a barrier of 13 kJ mol^{-1} was used for *p*-sulphamidoaniline and *p*-sulphoaniline.

DOI: 10.1002/poc

would also lie close together on the reaction coordinate. This conclusion agrees with the previous result derived from the Leffler equation, in which we assigned the transition state an ON—X bond order of 0.83. It follows that the nitrosation reaction intermediates are close in both energy and structure (bond order) to the transition state. However, for the resonance-stabilised aniline derivatives, the greater intrinsic barrier yields higher energy transition states, with the Hammond postulate subsequently predicting somewhat less product-like bond orders. This effect is in addition to the generally larger thermodynamic barriers for the resonance-stabilised substrates, resulting from the higher overall electron-withdrawing ability of these substrates, as indicated by their respective pK_a values.

Brønsted relationships and other LFER

As mentioned in the introduction, many groups of researchers have developed relationship via Brønsted plots between lnk_N and pK_a for a range of nitrosation reactions. According to the Leffler equation, lnk_N shows an almost linear relationship with ΔG^o_N for nitrosation reactions, which leads us to postulate that the linearity between lnk_N and pK_a is actually a result of a linear relationship between ΔG^o_N and pK_a.[23] We will now expand upon this observation.

A change of substrate in our nitrosation reaction affects the free energy change of the reaction through the term $(\Delta G^o_{f,ONS^+} - \Delta G^o_{f,S})$, which we can calculate from the free energy data, obtained from application of the Marcus equation (tabulated in the supplementary material). The free energy of formation of the species ONS^+ can be described as the sum of the free energies of formation of the species ON^+ and S, and the free energy of formation of the ON—S^+ bond. Mathematically, this is represented by Eqn (11), where $\Delta G^o_{f,ON-S^+}$ represents the free energy of formation of the ON—S^+ bond only. All reported bond energies in this study refer to relaxed bond energies, which are sometimes termed interaction energies. The relaxed bond energy is the sum of the rigid bond energy and the relaxation energy. The relaxation energy is the energy change arising from geometry relaxation following bond cleavage.

$$\Delta G^o_{f,ONS^+} = \Delta G^o_{f,S} + \Delta G^o_{f,ON^+} + \Delta G^o_{f,ON-S^+} \quad (11)$$

Subtracting $\Delta G^o_{f,S}$ from both sides of Eqn (11):

$$\Delta G^o_{f,ONS^+} - \Delta G^o_{f,S} = \Delta G^o_{f,ON^+} + \Delta G^o_{f,ON-S^+} \quad (12)$$

The basicity, or pK_a, of a substrate is defined with respect to the free energies of formation of two species, as illustrated in Eqn (13). As for the above, we may express the free energy of formation of SH^+ as the sum of the free energies of formation of S, H^+ (which is equal to zero) and the S—H^+ bond, as shown in Eqn (14).

$$-2.30RT\mathrm{p}K_a = \Delta G^o_{f,SH^+} - \Delta G^o_{f,S} \quad (13)$$

$$\Delta G^o_{f,SH^+} = \Delta G^o_{f,S} + \Delta G^o_{f,H^+} + \Delta G^o_{f,S-H^+} \quad (14)$$

Equating Eqns (13) and (14), and setting the free energy of formation of H^+ to zero, we obtain Eqn (15). This reveals that pK_a is proportional to the free energy of formation of the S—H^+ bond.

$$\Delta G^o_{f,S-H^+} = -2.30RT\mathrm{p}K_a \quad (15)$$

We now propose that the Brønsted relationships often observed during nitrosation reactions arise due to a linear relationship between the free energy of formation of the ON—S^+ bond, and that of the S—H^+ bond. This relationship compares two thermodynamic parameters, as opposed to the usual method of constructing Brønsted plots for nitrosation reactions, where kinetic parameters from one reaction series are compared to thermodynamic parameters from another. Our proposed relationship is presented in Eqn (16). The relationship derived above for the free energy of formation of the ON—S^+ bond has been substituted into Eqn (16) to yield Eqn (17).

$$\Delta G^o_{f,ON-S^+} = \beta(\Delta G^o_{f,S-H^+}) \quad (16)$$

$$\Delta G^o_{f,ONS^+} - \Delta G^o_{f,S} = \beta(\Delta G^o_{f,S-H^+}) + \Delta G^o_{f,ON^+} \quad (17)$$

The relationship represented by Eqn (17) is plotted in Fig. 4 for the transfer of the nitroso group to various aniline-derived substrates. Here, $\Delta G^o_{f,SH^+}$ has been calculated according to Eqn (15). The substrates have been divided into four classes: the electronic effect anilines, the electronic effect naphthylamines, the resonance-stabilised anilines (including naphthylamines) and *p*-sulphamidoaniline and *p*-sulphoaniline. For the electronic effect aniline substrates, we observe a good

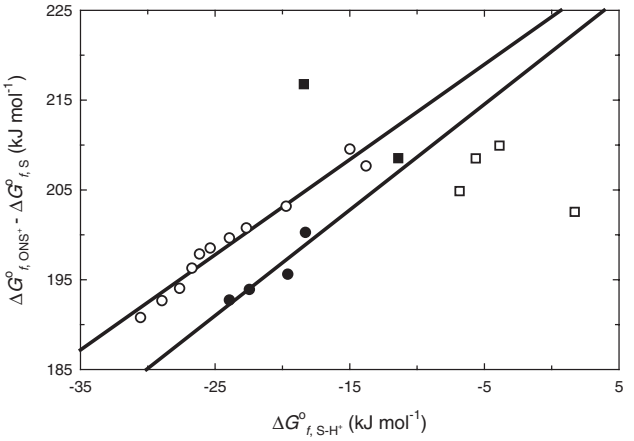

Figure 4. Relationship between nitroso species free energy and protonated amine free energy for a range of electronic effect anilines (○), electronic effect naphthylamines (●), resonance-stabilised anilines (□) and *p*-sulphoaniline and *p*-sulphamidoaniline (■)

DOI: 10.1002/poc

linear relationship, with a slope of 1.06 and intercept of $224\,kJ\,mol^{-1}$. The resemblance of the slope to unity indicates that, for the substrates tested, the ON—S^+ bond is thermodynamically similar to the corresponding S—H^+ bond. Furthermore, a slope of near-unity indicates that the slope arising from a Brønsted plot of $\ln k_N$ *versus* pK_a will be almost equivalent to that from a Leffler plot of ΔG^o *versus* $\Delta G^{\ddagger}_N$, for the nitrosation of the electronic-effect aniline derivatives. This result validates the use of Brønsted plots as indicators of $\alpha_{ON—S}$ for aniline nitrosation, though this approach would not necessarily be suitable for nitrosation of aniline derivatives substituted with π withdrawing groups, or with an extra aromatic ring. For the naphthylamine derivatives, we also observe a linear relationship, though with a slope of 1.18 and intercept of $220\,kJ\,mol^{-1}$. The remaining two groups did not fit either linear relationship. According to the intercepts of the linear relationships shown in Fig. 4, our model has predicted that the free energy of formation of ON^+ is equal to between 224 and $220\,kJ\,mol^{-1}$. This value compares well with the experimental value of $227\,kJ\,mol^{-1}$, which is deduced from the equilibrium constant for ON^+ formation measured by Becker *et al.*[37]

The equilibrium constant for NO^+ formation, in aqueous media, has been a point of considerable uncertainty. This equilibrium constant is relevant to acid catalysed nitrosation, where it has been argued that NO^+ is the effective nitrosating agent. Utilising the free energy of formation of NO^+ determined here, and published values[38] for HNO_2 ($-55.649\,kJ\,mol^{-1}$) and H_2O ($-237.129\,kJ\,mol^{-1}$), we have evaluated the equilibrium constant for NO^+ formation as between 3.6×10^{-8} and $1.8 \times 10^{-7}\,M^{-1}$. Comparatively, Becker *et al.*[37] measured this equilibrium constant to be $1.2 \times 10^{-8}\,M^{-1}$. Clearly, small changes in the free energy of formation of NO^+ have a dramatic effect on the equilibrium constant for NO^+ formation, due to the large absolute values of the free energies of formation of water and NO^+, and their relatively small summation. Other predictions for the equilibrium constant of aqueous NO^+ formation range from 3.0×10^{-5} to 7.8×10^{-9} (cited on page 6 of Ref. [13]).

The correlation observed in Fig. 4 suggests that nitroso group transfer to aniline derivatives occurs according to a charge-transfer controlled mechanism. However, this conflicts with the fact that the nitroso group is a soft acid, and as such should participate in mainly covalent bonding through frontier-controlled reactions. As such, we can conclude that the observed correlation in Fig. 4 is not actually a direct result of a charge-transfer controlled mechanism, but arises out of the resemblance of the property pK_a with E_n, over the narrow range of closely related substrates. This interpretation also accounts for the varied results of other researchers, who have only observed good linear Brønsted relationships for nitrosation reactions within narrow classes of related compounds. Edwards,[39] who first introduced the property E_n as a measure of nucleophilicity, noted that E_n contained some contribution from pK_a. Leffler and Grunwald[40] have also noted that some resemblance between pK_a and more traditional measures of nucleophilicity may arise when studying narrow series of related compounds. During a study of the methylation of 91 amines, Bunting *et al.*[41] observed that accurate Brønsted correlations could only be formulated if the amines were divided into a series of closely related structural classes. Importantly, this study, like ours, was concerned with substitution at a soft electrophilic centre, that is, a saturated carbon atom.

Considering the above, it may be concluded that nitroso group transfer does in fact take place according to a frontier-controlled mechanism, although apparent Brønsted relationships may exist within certain series of closely related compounds. For example, Brønsted relationships have been observed within reaction series consisting solely of primary amines, of secondary amines and of phenolate ions,[6b,d] but not for broader ranges of nucleophilic species.[8] Even in the present case, the linear correlation coefficient may be improved somewhat by narrowing the reaction series, and plotting only either the meta or para derivatives. Furthermore, the naphthylamine substrates obey an alternate linear relationship, while those substrates featuring π electron withdrawing substituents obey no clear relationship at all. This indicates that any major change in the electronic structure of the amino group (and not just its remote substituents) causes the Brønsted relationship to fail. Considering this, one should be careful not to place too much significance in the slope of Brønsted correlations arising from nitrosation reactions, as they hold little mechanistic significance. For example, one should not use them as indicators of bond order for the generation of More O'Ferrall–Jencks diagrams, unless one knows the fundamental relationship between the free energy of formation of the ON—S^+ bond and that of the S—H^+ bond, as shown in Fig. 4.

As noted, nitroso reactivity should, in theory, correlate better with parameters of nucleophilicity than with basicity. Radhakrishnamurti and Panigrahi[42] reported both Swain and Scott (n) and Edwards (E_n) nucleophilic parameters for certain aromatic amines in nitrobenzene–ethanol mixtures, which we may now use to correlate with the computed values of ($\Delta G^o_{f,ONS^+} - \Delta G^o_{f,S}$). The relevant nucleophilic constants are listed in Table 3, along with the basicity of each amine. Included in the table are n values calculated from the relationship of Korzhova *et al.*,[43] using their kinetic data for reaction with 1,3-diphenylpropynone in ethyl and tert-butyl alcohols. Both sets of n values have been plotted against ($\Delta G^o_{f,ONS^+} - \Delta G^o_{f,S}$) in Fig. 5, and good linear relationships are observed, similar to those obtained with pK_a. The two relationships do, however, possess different slopes, reflecting the two methods used to derive the different sets of nucleophilic parameters and the effects of

DOI: 10.1002/poc

Table 3. Basicity (pK_a), Swain and Scott nucleophilicity (n) and Edwards nucleophilicity (E_n) of certain aromatic amines

	pK_a	n	E_n
p-Methoxyaniline	5.36	4.79[43]	–
p-Methylaniline	5.08	4.8[42]; 4.57[43]	1.44
N-Methylaniline	4.85	4.9[42]	1.44
m-Methylaniline	4.69	4.7[42]; 4.50[43]	1.39
Aniline	4.59	4.5[42]; 4.34[43]	1.32
o-Methylaniline	4.45	4.3[42]; 4.32[43]	1.27
m-Methoxyaniline	4.20	4.33[43]	–
p-Chloroaniline	3.98	4.1[42]; 4.21[43]	1.22
m-Chloroaniline	3.46	3.9[42]	1.15

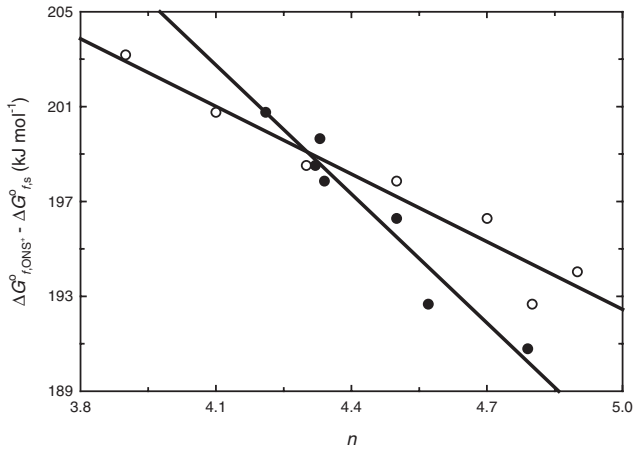

Figure 5. Relationships between amine nucleophilicity (n) and nitroso species free energy of formation for a range of aniline derivatives, using the nucleophilic data of Refs. [42] (○) and [43] (●)

the different solvents in which the reactions were carried out. When the reported E_n values are plotted against $(\Delta G^{o}_{f,ONS^+} - \Delta G^{o}_{f,S})$ as in Fig. 6, a slightly better linear relationship is obtained than the corresponding plot with pK_a (an R^2 value of 0.967, compared to 0.943 for the Brønsted plot). This supports our conclusion that the correlation between nitroso reactivity and basicity does not arise from the intrinsic reactivity of the system, but merely from the ability of basicity to mimic nucleophilicity, within a series of related compounds. However, the relationships featuring Swain and Scott nucleophilicity parameters do not improve upon the correlation coefficient of the Brønsted relationship, possibly due to inclusion of basicity effects in these parameters, and the effects of the non-aqueous solvents. Also included in Fig. 6 is a plot of Eqn (3), the relationship of da Silva *et al.*[14] relating the thermodynamics of nitroso transfer to E_n. The experimental results exhibit reasonable agreement with the thermodynamic relationship, though there is some difference in slope. We believe this difference largely arises from the systematic errors in the reported E_n

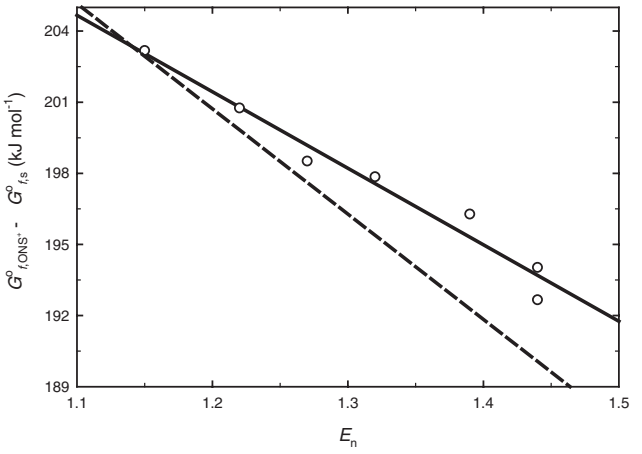

Figure 6. Relationship between E_n and nitroso species free energy of formation for a range of aniline derivatives, using the E_n parameters of Ref. [42]. The dotted line represents the relationship of Eqn (3)

values, as observed in Fig. 5. Significantly, however, the relationship of Eqn (3) would lie somewhere between the slopes of the two linear relationships depicted in Fig. 5.

Transition state and free energy profile analysis

Free energy profiles can be generated using the free energy data obtained via application of the Marcus equation, along with the known experimental free energies of activation. These free energy profiles show the relative free energies of the reaction products and reactants, and the position of the transition state. Free energy profiles have been created for the reaction of aniline with nitrosyl thiocyanate, using the free energy value provided in Table 2. The position of the transition state along the reaction coordinate (interpreted here as bond order, n) can be located in one of several ways. First, we could adopt a value of $n_T = 0.83$, as calculated earlier from the Leffler equation. However, this value only takes into account the position of the transition state relative to the nitrosating agent, and not the substrate, thus ignoring any deviations from synchronicity in the transition state. Another approach would be to attempt to quantitatively apply the Hammond postulate, via Eqn (18).[44]

$$n_T = \frac{1}{2 - \left(\frac{\Delta G^{o}}{\Delta G^{\ddagger}_{T}}\right)} \tag{18}$$

Equation (18) assumes that the reactants and the transition state, and the transition state and the products, are linearly connected, and the transition state lies upon the reaction coordinate at the position which minimises the distance traversed between the reactant and product states. For the nitrosation of aniline by nitrosyl

DOI: 10.1002/poc

thiocyanate, Eqn (18) predicts a transition state bond order of 0.97, which is somewhat greater than that suggested by the Leffler equation, though still indicative of a transition state that most resembles the reaction products. Another approach to locating the transition state, which again attempts to quantify the Hammond postulate, is to describe the product and reactant energies as harmonic parabolic wells.[45] The location of the transition state is then given by their point of intersection, and the parabolic barrier to the two wells may be taken as the free energy profile at the transition state. This profile will not describe the correct shape of the potential energy surface at either the reactant or the product states, but it will provide an accurate description around the transition state, which is the area of interest. In particular, this description will be more realistic than the linear profile assumed by Eqn (18). We have also calculated the free energy profile across the entire reaction using an average of the product and reactant free energy wells and the transition state free energy profile, linearly weighted according to the position along the reaction coordinate (i.e., using switching functions). At the transition state, the parabola describing the transition state free energy is given a weighting of one and the product and reactant parabolas are given a weighting of zero. These weightings are reversed at the product and reactant states.

Figure 7 shows a free energy profile for the reaction of aniline with nitrosyl thiocyanate, where we have arbitrarily assigned the free energy of the reactants to zero. The reactant and product energies have been described using harmonic wells, and are found to intersect at $n_T = 0.86$; this value agrees well with that predicted from the Leffler equation. It can be seen from the free energy profile that the reaction products are of relatively high energy, and the transition state is product-like. As a consequence of the low intrinsic barrier to reaction, the greatest impedance to reaction arises from the large thermodynamic barrier that must be traversed. In comparison, a free energy profile for the reaction of 4-nitro-1-naphthylamine with nitrosyl thiocyanate has also been constructed (Fig. 8), using an intrinsic barrier of $19\,\mathrm{kJ\,mol^{-1}}$, and the predicted ΔG^{o}_{N} value of $37.2\,\mathrm{kJ\,mol^{-1}}$. The bond order of the transition state was estimated to be 0.89 by Eqn (18), and 0.74 by the theory of intersecting harmonic parabolic wells. In this case, both the intrinsic barrier to reaction and the thermodynamic barrier to reaction are greater than those for aniline nitrosation, thus explaining the reduced rate of nitrosation.

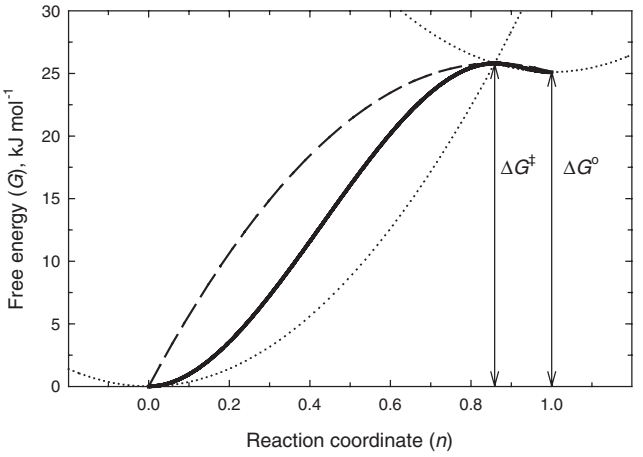

Figure 7. Free energy profile for the nitrosation of aniline by nitrosyl thiocyanate. Dotted lines represent harmonic parabolic wells situated at reactant and product free energies (reactant arbitrarily assigned to zero free energy). Dashed line represents the free energy profile at the transition state, calculated as the parabolic barrier to the two harmonic wells. The transition state is located at the intersection of the two harmonic wells

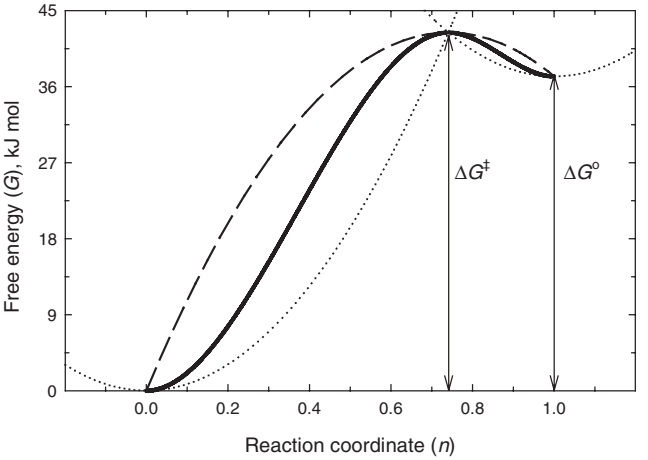

Figure 8. Free energy profile for the nitrosation of 4-nitro-1-naphthylamine by nitrosyl thiocyanate. Dotted lines represent harmonic parabolic wells situated at reactant and product free energies (reactant arbitrarily assigned to zero free energy). Dashed line represents the free energy profile at the transition state, calculated as the parabolic barrier to the two harmonic wells. The transition state is located at the intersection of the two harmonic wells

The amino group is π electron donating, because of its lone pair of electrons. In aniline (and its electronic-effect derivatives), there is some resonance donation through the aromatic ring, but the lone pair of electrons remains essentially intact (for a detailed discussion of the theoretical underpinnings of substituent effects in anilines and benzenes, see Ref. 46). Consequently, *N*-nitrosation would not involve significant resonance stabilisation in the diazo bond, only formation of a σ covalent bond. Because electron transfer and covalent σ bond formation are much more rapid processes than resonance stabilisation and charge delocalisation,[47] formation of the ON—S bond occurs quickly, and at about the same rate as cleavage of the ON—X bond. This explains the relatively low intrinsic barrier to reaction.

For the resonance-stabilised aniline derivatives, the π donating amino group can undergo interaction with the π withdrawing substituent (e.g. the nitro group), through the

DOI: 10.1002/poc

aromatic ring. Subsequently, delocalisation of the amino group lone pair into the aromatic ring occurs. Structurally, a double Ph $=$ NH_2 bond is formed, while the structure of the amine group transforms from a pyramidal to a planar geometry. By removing the lone pair the reactive site on the amine group is altered (both electronically and structurally), slowing the reaction rate by increasing the intrinsic barrier to reaction. In the case of lone pair delocalisation, one would expect no appreciable change in the rate of ON—X cleavage, thus resulting in a less synchronous reaction pathway than that observed for nitrosation of the electronic-effect derivatives. Furthermore, the amino group rearranges from a planar geometry in the reactant to a pyramidal geometry in the produced nitrosamine, providing a further energy barrier for the transition state to traverse.

The free energy data calculated according to the Marcus equation (Table 2) can also be used to estimate the structure (i.e. bond order) of the transition state with respect to the substrate, $\alpha_{ON—S}$. According to Eqn (6), this requires a plot of ΔG_N^o *versus* $\Delta G_N^{\ddagger}$ for the nitrosation of a range of substrates by one particular nitrosating agent. Plots of ΔG_N^o *versus* $\Delta G_N^{\ddagger}$ have been made for the nitrosating agents N_2O_3, ONI, ONSCN and ON^+SC $ON^+SC(NH_2)_2$, and respective slopes of 0.79, 0.81, 0.93 and 0.88 were obtained, yielding an average slope of 0.85. The plots of ΔG_N^o *versus* $\Delta G_N^{\ddagger}$ are included as supplementary material, showing that accurate linear relationships were obtained in all cases. The $\alpha_{ON—S}$ value calculated here may be used along with the earlier calculated $\alpha_{ON—X}$ value to build a More O'Ferrall–Jencks diagram.[48] This diagram is shown in Fig. 9, where $n_{ON—X}$ has been used to designate the order of the cleaving ON—X bond, and $n_{ON—S}$ to designate the order of the forming ON—S bond. The More O'Ferrall–Jencks plot illustrates that the transition state is synchronously well balanced, and that a concerted reaction mechanism is followed. In Fig. 9, the transition state bond order with respect to both the substrate and nitrosating agent is 0.84, compared to the intersecting parabolic wells prediction of 0.86.

We have also attempted to create a More O'Ferrall–Jencks diagram for the nitrosation of the resonance-stabilised aniline derivatives, to compare with that for the other aniline compounds. However, this task was made difficult by the lack of experimental data for this reaction series. Initially, a value for $\alpha_{ON—X}$ was estimated from the plot of $\ln k_N$ against E_n for the nitrosation of 4-nitro-1-naphthylamine by a range of nitrosating agents (supplementary material). A slope of -13.1 was obtained, providing an $\alpha_{ON—X}$ value of 0.74. This value is, as expected, relatively similar to that found for nitrosation of the electronic-effect aniline compounds. To estimate $\alpha_{ON—S}$ we must compare nitrosation measurements across a range of substrates, however, such measurements only exist for nitrosation via nitrosyl bromide. Consequently, a less accurate estimate of $\alpha_{ON—S}$ is made, compared to the electronic-effect substrates. A plot was made between ΔG_N^o and $\Delta G_N^{\ddagger}$ for nitrosation of the substrates by ONBr (see supplementary material), and a resultant slope of 0.50 was obtained. The overall transition-state bond order is thus predicted as 0.66, compared to a prediction of 0.74 from the intersecting parabolic wells. For interest sake, an evaluation of $\alpha_{ON—S}$ for *p*-sulphamidoaniline and *p*-sulphoaniline results in a value of 0.82, which lies between the respective

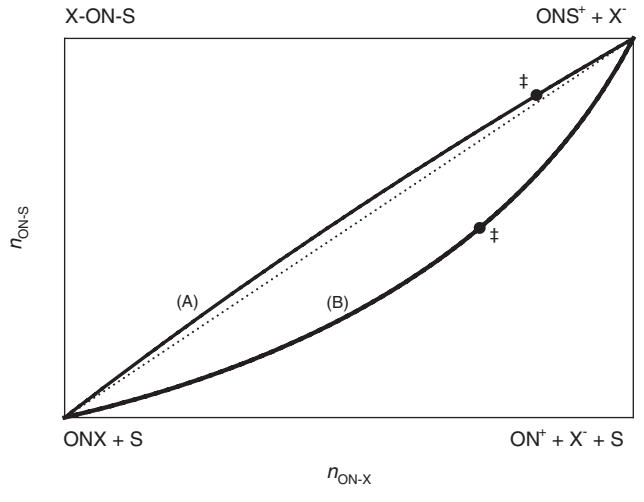

Figure 9. More O'Ferrall–Jencks diagram for (A) electronic-effect aniline nitrosation and (B) resonance-stabilised aniline nitrosation. Solid lines represent the actual reaction pathways, where the solid circles indicate the positions of the transition states. The dashed line represents the hypothetical pathway for the pure concerted reaction

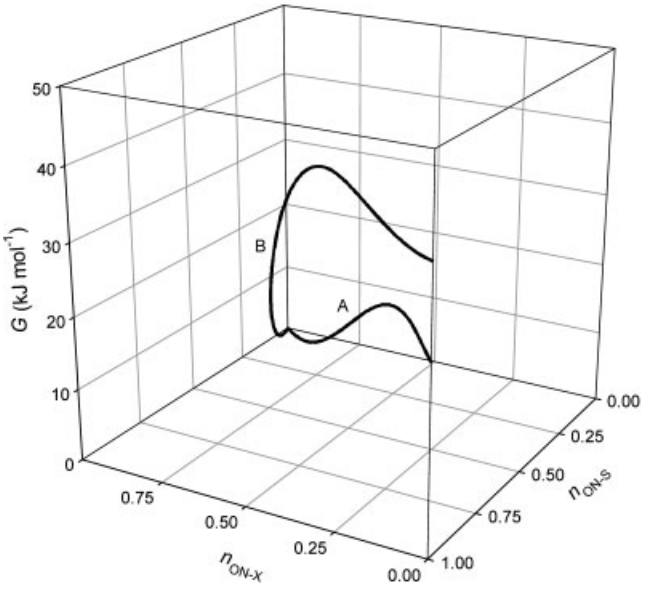

Figure 10. Optimum reaction pathway through the free energy surface for (A) the nitrosation of aniline and (B) the nitrosation of 4-nitro-1-naphthylamine by nitrosyl thiocyanate

DOI: 10.1002/poc

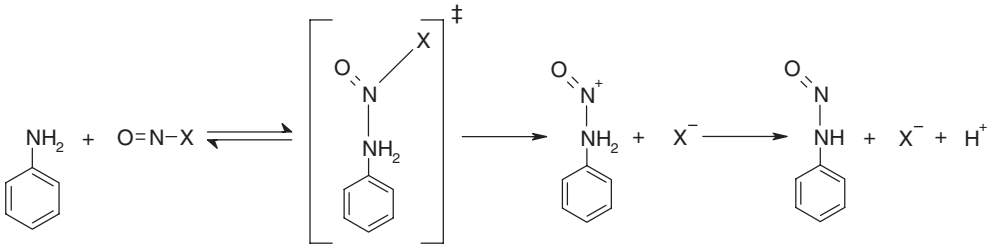

Figure 11. Schematic representation of the reaction mechanism for aniline nitrosation by a general nitrosating agent (ONX)

electronic-effect and resonance-stabilised values, supporting our earlier conclusion that only a weak resonance effect is active for these two substrates.

Figure 9 shows the More O'Ferrall–Jencks diagram resulting from the determined values of $\alpha_{ON—X}$ and $\alpha_{ON—S}$ for resonance-stabilised and electronic-effect aniline nitrosation. This figure confirms that the transition state for resonance-stabilised aniline nitrosation is less synchronous than that for general aniline nitrosation, and that the transition state occurs earlier along the reaction coordinate.

From the free energy profiles and the More O'Ferrall–Jencks diagrams we obtain both the reaction path between reactants and products and the free energy at each point along this path. Combining these two sets of information, we can generate three-dimensional plots depicting the optimal reaction path on the free energy surface. Figure 10 shows the reaction paths for the nitrosation of aniline and 4-nitro-1-naphthylamine by nitrosyl thiocyanate, arrived at by combining Fig. 9 with Figs. 7 and 8, respectively. Figure 10 illustrates the relationship between the increasing thermodynamic and intrinsic barriers, and the loss of synchronicity in the transition state. According to the preceding analyses, the general mechanism being followed during electronic-effect aniline nitrosation is depicted in Fig. 11.

CONCLUSIONS

We have undertaken a comprehensive study of nitroso transfer to a wide range of aniline derivatives, with the findings summarised as follows:

(1) The Marcus equation has been used to correlate the free energy change for nitrosation with the free energy of activation. The quadratic form of the Marcus equation accounts for departures from linearity witnessed using the Leffler equation. From a simultaneous iterative solution of the resultant correlation, an intrinsic barrier to reaction of $10\,kJ\,mol^{-1}$ was calculated. This value indicates that nitroso reactivity is limited mostly by thermodynamics, not the intrinsic reactivity of the system. For the nitrosation of resonance-stabilised aniline derivatives, an increased intrinsic barrier of $19\,kJ\,mol^{-1}$ was estimated.

(2) A linear relationship has been developed between $\ln k_N$ and E_n according to the Leffler equation, which has proven to hold for nitrosation by all but the least reactive (least electrophilic) nitrosating agents. The slope of the relationship indicates that the transition state species in nitrosation reactions of this type largely resembles the reaction products.

(3) A linear relationship was demonstrated between the free energies of formation of nitrosamines and their corresponding protonated amines. This relationship mirrors the so-called Brønsted relationships, which are generally taken to indicate the existence of charge-transfer controlled reactions. However, this is not the case with the present result, where the observed relationship merely arises out of the similarity of the amines examined. Nitroso reactivity was found to correlate better with the nucleophilic parameters of Swain and Scott, and Edwards.

(4) Nitrosation of aniline and its derivatives was shown to proceed via a concerted mechanism, with a synchronously well-balanced transition state, by way of a More O'Ferrall–Jencks diagram. This finding agrees with the relatively low intrinsic barrier to reaction determined through the Marcus equation. However, for the nitrosation of resonance-stabilised derivatives, the larger intrinsic barrier resulted in a less synchronous transition state, where formation of the ON—S bond was slow in comparison to cleavage of the ON—X bond. We attributed this to significant resonance stabilisation induced by interaction of the π accepting substituent with the aromatic ring, thus isolating a π electron on the amino group.

SUPPLEMENTARY MATERIAL

Table of calculated values of $(\Delta G^{o}_{f,ONS^{+}} - \Delta G^{o}_{f,S})$ $(kJ\,mol^{-1})$ for a range of aniline derivatives. Plot of ΔG^{o}_{N} *versus* $\Delta G^{\ddagger}_{N}$ for the nitrosation of electronic-effect aniline derivatives by the nitrosating agents dinitrogen trioxide, nitrosyl iodide, nitrosyl thiocyanate and

DOI: 10.1002/poc

S-nitrosothiourea. Plot of $\ln k_N$ against E_n for the nitrosation of 4-nitro-1-naphthylamine by a range of nitrosating agents. Plot of ΔG^o_N *versus* ΔG_N for the nitrosation of resonance-stabilised aniline derivatives by the nitrosating agent nitrosyl bromide.

Acknowledgements

We would like to thank the Australian Research Council for providing a postgraduate scholarship to G D, and Orica Australia for project funding. The Australian Research Council and Orica Explosives Australia Pty, Ltd.

REFERENCES

1. Butler AR, Williams DLH. *Chem. Soc. Rev.* 1993; 233–241.
2. Magee PN, Barnes JM. *Brit. J. Cancer* 1956; **10**: 114–122.
3. (a) da Silva G, Dlugogorski BZ, Kennedy EM. *Chem. Eng. Sci.* 2006; **61**: 3186–3197 (available online Jan. 24, 2006. DOI: 10.1016/j.ces.2005.11.059); (b) da Silva G, Dlugogorski BZ, Kennedy EM. *AIChE J.* 2006; **52**: 1558–1565; (c) Nguyen DA, Iwaniw MA, Fogler HS. *Chem. Eng. Sci.* 2003; **58**: 4351–4362.
4. (a) Bartberger MD, Mannion JD, Powell SC, Stamler JS, Houk KN, Toone EJ. *J. Am. Chem. Soc.* 2001; **123**: 8868–8869; (b) Bartsch RA, Chae YM, Ham S, Birney DM. *J. Am. Chem. Soc.* 2001; **123**: 7479–7486; (c) Cheng J, Xian M, Wang K, Zhu X, Yin Z, Wang PG. *J. Am. Chem. Soc.* 1998; **120**: 10266–10267; (d) da Silva G, Kennedy EM, Dlugogorski BZ. *J. Phys. Chem. A* 2007; **111**: 1300–1306; (e) Fu Y, Mou Y, Lin B, Liu L, Guo Q. *J. Phys. Chem. A* 2002; **106**: 12386–12392; (f) Lü J, Wittbrodt JM, Wang K, Wen Z, Schlegel B, Wang PG, Cheng J. *J. Am. Chem. Soc.* 2001; **123**: 2903–2904.
5. (a) Gwaltney SR, Rosokha SV, Head-Gordon M, Kochi JK. *J. Am. Chem. Soc.* 2003; **125**: 3273–3283; (b) Leach AG, Houk KN. *Org. Biomol. Chem.* 2003; **1**: 1389–1403; (c) Reynolds CA, Thomson C. *J. Chem. Soc. Perkin Trans.* 1987; **2**: 1337–1340; (d) Skokov S, Wheeler RA. *J. Phys. Chem. A* 1999; **103**: 4261–4269; (e) Zhu X, He J, Li Q, Xian M, Lu J, Cheng J. *J. Org. Chem.* 2000; **65**: 6729–6735.
6. (a) García-Río L, Leis JR, Moreira JA, Serantes D. *Eur. J. Org. Chem.* 2004; 614–622; (b) García-Río L, Leis JR, Moreira JA, Norberto F. *J. Org. Chem.* 2001; **66**: 381–390; (c) Leis JR, Peña ME, Ríos A. *J. Chem. Soc., Perkin Trans. 2* 1993; 1233–1240; (d) Leis JR, Ríos A. *J. Chem. Soc. Perkin Trans. 2* 1996; 857–863; (e) Leis JR, Ríos A, Rodríguez-Sánchez L. *J. Chem. Soc., Perkin Trans. 2* 1998; 2729–2734; (f) Stedman G, Whincup PAE. *J. Chem. Soc.* 1963; 5796–5799.
7. Calle E, Casado J, Cinos JL, Mateos FJG, Tostado M. *J. Chem. Soc., Perkin Trans. 2* 1992; 987–991.
8. García-Río L, Iglesias E, Leis JR, Peña ME, Ríos A. *J. Chem. Soc. Perkin Trans. 2* 1993; 29–37.
9. (a) Leis JR, Peña ME, Ríos AM. *J. Chem. Soc. Perkin Trans. 2* 1995; 587–593; (b) Munro AP, Williams DLH. *J. Chem. Soc., Perkin Trans. 2* 1999; 1989–1993.
10. (a) Darbeau RW, Pease RS, Gibble RE. *J. Org. Chem.* 2001; **66**: 5027–5032; (b) Darbeau RW, Pease RS, Perez EV. *J. Org. Chem.* 2002; **67**: 2942–2947; (c) García-Río L, Leis JR, Moreira JA, Norberto F. *J. Chem. Soc., Perkin Trans. 2* 1998; 1613–1620; (d) Isobe M. *Bull. Chem. Soc. Jpn.* 1985; **58**: 2844–2848; (e) Williams DLH. *J. Chem. Soc., Perkin Trans. 2* 1977; 502–504.
11. Thompson JT, Williams DLH. *J. Chem. Soc., Perkin Trans. 2* 1977; 1932–1937.
12. (a) Singer SS. *J. Org. Chem.* 1978; **43**: 4612–4616; (b) Singer SS, Singer GM, Cole BB. *J. Org. Chem.* 1980; **45**: 4931–4935.
13. Williams DLH. *Nitrosation*. Cambridge University Press: Cambridge, 1988; 17–18.
14. da Silva G, Kennedy EM, Dlugogorski BZ. *J. Chem. Res. (S)* 2002; 589–590.
15. Ridd JH. *Quart. Rev. (London)* 1961; **15**: 418–441.
16. Schmid H, Hallaba E. *Monatsh. Chem.* 1956; **87**: 560–573.
17. Schmid H, Fouad MG. *Monatsh. Chem.* 1957; **88**: 631–638.
18. Dozsa L, Szilassy I, Beck MT. *Inorg. Chim. Acta.* 1976; **17**: 147–153.
19. Al-Mallah K, Collings P, Stedman G. *J. Chem. Soc., Dalton Trans.* 1974; 2469–2472.
20. (a) Abia L, Castro A, Iglesias E, Leis JR, Peña , ME. *J. Chem. Res. (S)* 1989; 106–107; (b) Garley MS, Stedman G. *J. Inorg. Nucl. Chem.* 1981; **43**: 2863–2867.
21. Markovits GY, Schwartz SE, Newman L. *Inorg. Chem.* 1981; **20**: 445–450.
22. (a) Aboul-Seoud A, Ahmad MI. *J. Prakt. Chem.* 1978; **320**: 1012–1016; (b) Aboul-Seoud A, Mansour IAS, Fawzy WM. *Afinidad* 1981; **38**: 23–27; (c) Bryant T, Williams DLH, Ali MHH, Stedman G. *J. Chem. Soc., Perkin Trans. 2* 1986; 193–196; (d) Casado J, Castro A, Iglesias E, Peña ME, Tato JV. *Can. J. Chem.* 1986; **64**: 133–137; (e) Castro A, Iglesias E, Leis JR, Peña ME. *Ber. Bunsenges. Phys. Chem.* 1986; **90**: 891–895; (f) Crampton MR, Thompson JT, Williams DLH. *J. Chem. Soc., Perkin Trans. 2* 1979; 18–22; (g) Dix LR, Williams DLH. *J. Chem. Res. (S)* 1984; 96–97; (h) Fitzpatrick J, Meyer TA, O'Neill ME, Williams DLH. *J. Chem. Soc., Perkin Trans. 2* 1984; 927–932; (i) Keizer J. *Chem. Rev.* 1987; **87**: 167–180; (j) Ridd JH. *Adv. Phys. Org. Chem.* 1978; **16**: 1–49; (k) Schmid H, Essler C. *Monatsh. Chem.* 1958; **88**: 1110–1112.
23. da Silva G, Kennedy EM, Dlugogorski BZ. *Ind. Eng. Chem. Res.* 2004; **43**: 2296–2301.
24. Edwards JO. *J. Am. Chem. Soc.* 1954; **76**: 1540–1547.
25. Klopman G. *J. Am. Chem. Soc.* 1968; **90**: 223–234.
26. Pearson RG. *J. Am. Chem. Soc.* 1963; **84**: 3533–3539.
27. Yingst A, McDaniel DH. *Inorg. Chem.* 1967; **6**: 1067–1068.
28. (a) Leffler JE. *Science* 1953; **117**: 340–341; (b) Marcus RA. *J. Chem. Phys.* 1956; **24**: 966–978; (c) Marcus RA. *J. Phys. Chem.* 1968; **72**: 891–899.
29. Bernasconi CF. *Acc. Chem. Res.* 1992; **25**: 9–16.
30. da Silva G, Kennedy EM, Dlugogorski BZ. *J. Am. Chem. Soc.* 2005; **127**: 3664–3665.
31. (a) Bernasconi CF. *Acc. Chem. Res.* 1987; **20**: 301–308; (b) Eliad L, Hoz S. *J. Phys. Org. Chem.* 2002; **15**: 540–543.
32. Bernasconi CF. *Tetrahedron* 1985; **41**: 3219–3234.
33. Murdoch JR. *J. Phys. Chem.* 1983; **87**: 1571–1579.
34. Saunders WH, Jr. *J. Phys. Chem.* 1982; **86**: 3321–3323.
35. Cohen AO, Marcus RA. *J. Phys. Chem.* 1968; **72**: 4249–4256.
36. Hubig SM, Kochi JK. *J. Am. Chem. Soc.* 2000; **122**: 8279–8288.
37. Becker KH, Kleffmann J, Kurtenbach R, Wiesen P. *J. Phys. Chem.* 1996; **100**: 14984–14990.
38. Wagman DD, Evans WH, Parker VB, Halow I, Bailey SM, Schumm RH. *NBS Technical Note 270-3*, National Bureau of Standards: Washington, D. C., 1968.
39. Edwards JO. *J. Am. Chem. Soc.* 1956; **78**: 1819–1820.
40. Leffler JE, Grunwald E. *Rates and Equilibria of Organic Reactions*. John Wiley and Sons, Inc: New York, 1963; 236–237.
41. Bunting JW, Mason JM, Heo CKM. *J. Chem. Soc., Perkin Trans. 2* 1994; 2291–2300.
42. Radhakrishnamurti PS, Panigrahi GP. *J. Indian Chem. Soc.* 1969; **46**: 318–322.
43. Korzhova N, Pisareva VS, Unikovskaya LV, Korshunov SP. *Osnovn. Org. Sint. Neftekhim.* 1975; 99–105.
44. Agmon N. *J. Chem. Soc. Faraday Trans.* 1977; **52**: 197–201.
45. Kurz J. *Chem. Phys. Lett.* 1978; **57**: 243–246.
46. Pross A, Radom L. *Adv. Phys. Org. Chem.* 1981; 1–61.
47. Bernasconi CF. *Adv. Phys. Org. Chem.* 1992; **27**: 119–238.
48. (a) Jencks WP. *Chem. Revs.* 1972; **72**: 705–718; (b) Jencks DA, Jencks WP. *J. Am. Chem. Soc.* 1977; 7948–7960; (c) More O'Ferrall RA. *J. Chem. Soc. (B)* 1970; 274–277.

DOI: 10.1002/poc